

Signatures of Non-universal Quantum Dynamics of Ultracold Chemical Reactions of Polar Alkali Dimer Molecules with Alkali Metal Atoms: $\text{Li}({}^2\text{S}) + \text{NaLi}(\sigma{}^3\Sigma^+) \rightarrow \text{Na}({}^2\text{S}) + \text{Li}_2(\sigma{}^3\Sigma_u^+)$

Masato Morita, Brian K. Kendrick, Jacek Kłos, Svetlana Kotochigova, Paul Brumer,* and Timur V. Tscherbul*



Cite This: *J. Phys. Chem. Lett.* 2023, 14, 3413–3421



Read Online

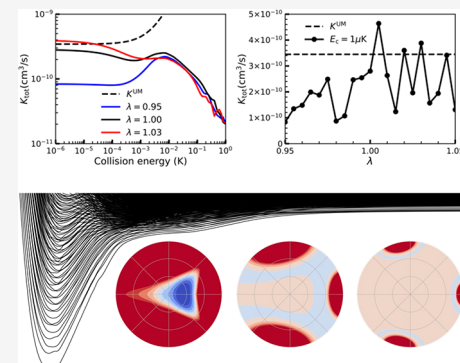
ACCESS |

Metrics & More

Article Recommendations

Supporting Information

ABSTRACT: Ultracold chemical reactions of weakly bound triplet-state alkali metal dimer molecules have recently attracted much experimental interest. We perform rigorous quantum scattering calculations with a new *ab initio* potential energy surface to explore the chemical reaction of spin-polarized $\text{NaLi}(\sigma{}^3\Sigma^+)$ and $\text{Li}({}^2\text{S})$ to form $\text{Li}_2(\sigma{}^3\Sigma_u^+)$ and $\text{Na}({}^2\text{S})$. The reaction is exothermic and proceeds readily at ultralow temperatures. Significantly, we observe strong sensitivity of the total reaction rate to small variations of the three-body part of the Li_2Na interaction at short range, which we attribute to a relatively small number of open $\text{Li}_2(\sigma{}^3\Sigma_u^+)$ product channels populated in the reaction. This provides the first signature of highly non-universal dynamics seen in rigorous quantum reactive scattering calculations of an ultracold exothermic insertion reaction involving a polar alkali dimer molecule, opening up the possibility of probing microscopic interactions in atom+molecule collision complexes via ultracold reactive scattering experiments.



The study of chemical reactions at low and ultralow temperatures is projected to create major advances in our understanding of chemical reactivity at the most fundamental level.^{1–5} The large de Broglie wavelength of ultracold molecular reactants² combined with the experimenter's ability to prepare them in single well-defined quantum states give rise to pronounced quantum effects, making ultracold chemical reactions an ideal platform for exploring the impact of these fascinating effects on chemical reactivity. Examples include threshold and resonance scattering,^{3,6–8} quantum reflection,^{9–11} quantum statistics,^{12,13} and quantum coherent control.^{14,15} In addition, the detection of reaction products and intermediate collision complexes has been experimentally realized,^{16,17} enabling precision tests of long-held statistical theories of chemical dynamics.¹⁸

All chemical reactions studied thus far at low and ultralow temperatures can be classified into abstraction and insertion types.^{19,20} Abstraction reactions, such as $\text{F} + \text{H}_2 \rightarrow \text{HF} + \text{H}$ ^{21–23} and $\text{H(D)} + \text{H}_2 \rightarrow \text{H}_2(\text{HD}) + \text{D}$,^{24–28} possess an activation barrier, whereas insertion reactions, such as $\text{K} + \text{KRb} \rightarrow \text{K}_2 + \text{Rb}$ ^{29,30} and $\text{KRB} + \text{KRb} \rightarrow \text{K}_2 + \text{Rb}_2$,^{18,31} are barrierless and characterized by a deep potential well.³²

Ultracold insertion reactions are generally described well by universal models (UMs),^{13,18,29,33–36} which assume that once the reactants approach each other at close range, they react with unit probability. Exact quantum dynamics calculations showed that the rate of the $\text{K} + \text{KRb}(\text{X}^1\Sigma^+)$ chemical reaction is in excellent agreement with the UM prediction²⁹ and with

experiment.³¹ For other insertion chemical reactions, such as $\text{Li} + \text{YbLi}(\text{X}^2\Sigma^+) \rightarrow \text{Li}_2(\text{X}^1\Sigma_g^+) + \text{Yb}$ ^{37,38} and $\text{Li} + \text{NaLi}(\text{X}^1\Sigma^+) \rightarrow \text{Li}_2(\text{X}^1\Sigma_g^+) + \text{Na}$,^{39,40} the calculated deviations from the UM do not exceed 30%.

While UMs are an important tool,^{34,35,41} they do not provide insight into microscopic interactions within the reaction complex,⁶ which is crucial for designing mechanisms for controlling the reaction dynamics via, e.g., scattering resonances.^{6,42} Similarly, they provide no information about conditions for the validity of UMs or the parameter dependence of the dynamics. Hence, identifying systems showing significant deviations from universal behavior (non-universal effects) is an important goal, which can yield insights into short-range interactions in the reaction complex and enable one to tune ultracold chemical reactivity with scattering resonances, a long sought-after goal of ultracold chemistry.^{3,43} Signatures of non-universal effects were observed experimentally in ultracold collisions of Li_2 Feshbach molecules with Li atoms⁴⁴ and, very recently, in ground rovibrational-state molecule–atom and molecule–molecule collisions, such as K

Received: January 17, 2023

Accepted: March 24, 2023

Published: March 31, 2023



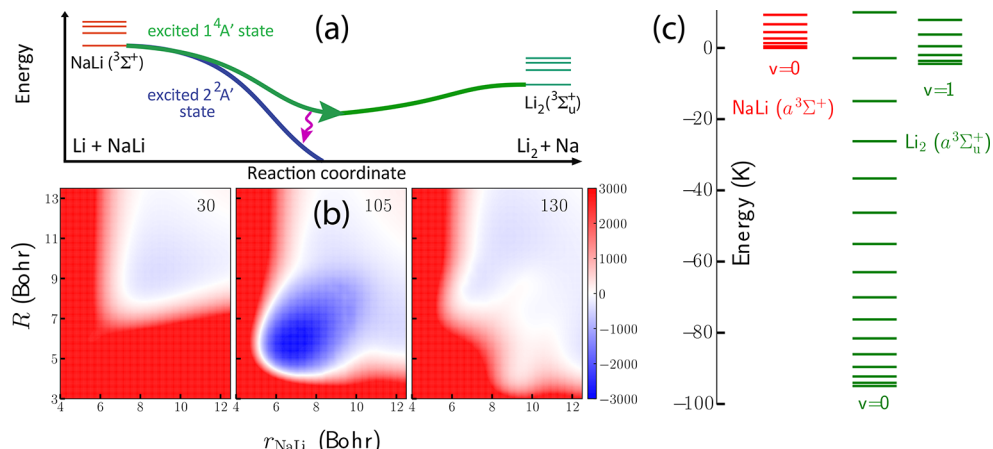


Figure 1. (a) Schematic diagram of the chemical reaction $\text{Li} + \text{NaLi}(a^3\Sigma^+) \rightarrow \text{Li}_2(a^3\Sigma_u^+) + \text{Na}$. The reaction of spin-polarized reactants proceeds via a spin-conserving pathway on the high-spin $1^4A'$ PES (green line) as predicted by the Wigner spin rule. The spin-nonconserving reaction pathway forbidden by the Wigner spin rule (not considered in this work) requires a non-adiabatic transition to the excited $2^2A'$ PES (wavy line). (b) *Ab initio* PES for the $1^4A'$ electronic state of the Li_2Na trimer computed in this work plotted as a function of the Jacobi coordinates (R , r_{NaLi}) at Jacobi angles (θ) of 30° (left), 105° (middle), and 130° (right) in the $\text{Li} + \text{NaLi}$ arrangement. (c) Energy diagram for the rovibrational states of the $\text{LiNa}(a^3\Sigma^+)$ reactant and $\text{Li}_2(a^3\Sigma_u^+)$ product. Zero energy corresponds to the energy of the rovibrational ground state of $\text{LiNa}(a^3\Sigma^+, v = 0, j = 0)$.

+ NaK($X^1\Sigma^+$),⁴⁵ Na + NaLi($a^3\Sigma^+$),⁸ and NaLi + NaLi,⁴⁶ where the observed reaction rate coefficients deviate from UM predictions by several orders of magnitude. The ultracold chemical reaction of polar NaLi($a^3\Sigma^+$) molecules with Li atoms to form the $\text{Li}_2(a^3\Sigma_u^+) + \text{Na}$ products is a natural candidate for searching for non-universal effects, as it is energetically allowed [unlike the $\text{Na} + \text{NaLi}(a^3\Sigma^+) \rightarrow \text{Na}_2(a^3\Sigma_u^+) + \text{Li}$ reaction⁷], experimentally feasible,^{8,47,48} and amenable to rigorous theoretical studies due to light reactants.

Non-universal behavior has not yet been seen in rigorous quantum scattering calculations on ultracold chemical reactions of polar alkali dimers. Such behavior has been predicted for only ultracold reactions of nonpolar molecules, such as $\text{Li} + \text{Li}_2(a^3\Sigma_u^+)$,^{49,50} Na + Na₂($a^3\Sigma_u^+$),⁵¹ K + K₂($a^3\Sigma_u^+$),⁵² and ${}^7\text{Li} + {}^6\text{Li}^7\text{Li} \rightarrow {}^7\text{Li}_2 + {}^6\text{Li}$.⁵³ These reactions are unique in that (i) they have a vanishingly small exothermicity, so only a few product states are populated at ultralow temperatures,⁵⁴ and (ii) their reactants and products are identical (apart from isotopic substitution). As a result, their zero-temperature rates tend to be below the universal values, on the order of $4.7 \times 10^{-12} \text{ cm}^3/\text{s}$ for the ${}^7\text{Li} + {}^6\text{Li}^7\text{Li}$ reaction,⁵⁴ and may not be detectable experimentally. In the most thoroughly studied cases in which the reactants and products are identical, it is not even possible to disentangle chemical reactivity from inelastic processes.⁵⁴ By contrast, ultracold chemical reactions probed in recent experiments^{8,48} involve polar triplet-state alkali dimers (such as NaLi) and can be exothermic by several hundreds of kelvin, potentially populating dozens of product rovibrational states.

Here, we show that pronounced non-universal effects can occur in the ultracold insertion reaction of spin-polarized triplet NaLi molecules and Li atoms, $\text{Li}({}^2S) + \text{NaLi}(a^3\Sigma^+, v = 0, j = 0) \rightarrow \text{Li}_2(a^3\Sigma_u^+, v', j') + \text{Na}({}^2S)$, significantly extending the range of systems displaying non-universal behavior. We use rigorous quantum scattering calculations based on our *ab initio* interaction potentials to map out the dependence of the reaction rates on the incident collision energy. Our calculations show that the reaction occurs at a high rate, and hence, it can be detected experimentally in an ultracold spin-polarized Li/NaLi mixture. In addition, the total reaction rate is sensitive to

small variations of the short-range part of the interaction potential even after summing over all state-to-state reaction rates and can deviate by a factor of ≈ 4 from the UM prediction, representing the first rigorous theoretical demonstration of non-universal behavior in an ultracold insertion reaction involving a polar molecule. (Note that the non-universal behavior recently observed in ultracold K + NaK, Na + NaLi, and NaLi + NaLi collisions^{8,45,46} is not yet amenable to rigorous quantum scattering calculations due to the large density of rovibrational states of the reactants, non-adiabatic effects, and external fields present in these experiments.) We attribute this highly non-universal behavior to a relatively low density of resonance states in this reaction and a limited number of open product channels compared to the chemical reactions explored previously,^{29,37–40} which displayed close to universal behavior. Our results suggest that non-universal effects can be experimentally observed in ultracold chemical reactions of spin-polarized triplet-state alkali metal dimers with alkali metal atoms. This opens up the prospects of mapping atom–molecule interactions within the reaction complex and of controlling the reaction dynamics with external fields, motivating further experimental and theoretical research into non-universal ultracold chemistry.

We consider the chemical reaction of ${}^{23}\text{Na}{}^6\text{Li}$ molecules in their metastable triplet electronic states $a^3\Sigma^+$, created in recent experiments.⁴⁷ Figure 1a shows a schematic of the reaction path of the $\text{Li}({}^2S) + \text{NaLi}(a^3\Sigma^+) \rightarrow \text{Li}_2(a^3\Sigma_u^+) + \text{Na}({}^2S)$ reaction. The 3-fold spin degeneracy of NaLi($a^3\Sigma^+$) and the 2-fold spin degeneracy of $\text{Li}({}^2S)$ give rise to two adiabatic potential energy surfaces (PESs) of doublet ($2^2A'$, $S = 1/2$) and quartet ($1^4A'$, $S = 3/2$) symmetries, where S is the total spin of the reaction complex. The PESs are split at short range by a strong spin exchange interaction. While the high-spin $1^4A'$ PES is the lowest state in the quartet symmetry, the doublet $2^2A'$ is the first excited state in the doublet spin symmetry. The ground-state $1^2A'$ PES (not shown in Figure 1a) correlates with the $\text{Li}({}^2S) + \text{NaLi}(X^1\Sigma^+)$ reactants in their ground electronic states,³⁹ which lie 9629 K below the $\text{Li}({}^2S) + \text{NaLi}(a^3\Sigma^+)$ asymptote of interest here. The ground and first excited doublet PESs exhibit a conical intersection (CI), which

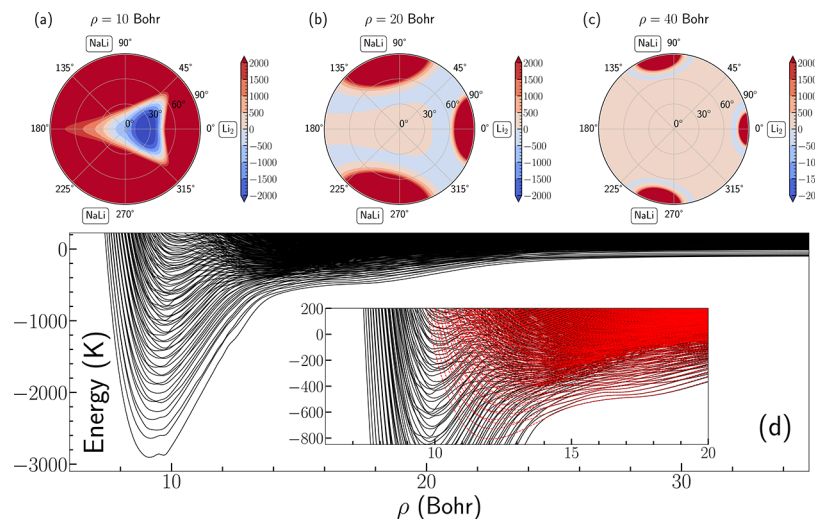


Figure 2. (a–c) Stereographic projections of the $ab\ initio$ $1^4A'$ PES of the NaLi_2 trimer for several values of hyperradius (in a_0): $\rho = 10$, $\rho = 20$, and $\rho = 40$, respectively. The north pole of the hypersphere is centered at the origin, and the zero energy is chosen at the rovibrational ground state of the NaLi reactant. The region of configurational space accessible at ultralow energies is colored blue. (d) Adiabatic potential curves as a function of ρ for $J = 0^+$ and even exchange symmetry of Li nuclei. The inset shows the adiabatic curves in the vicinity of the reactant threshold. The adiabats calculated without the three-body interaction are shown by the red (light gray) dashed lines.

has a pronounced effect on the quantum dynamics of the ultracold chemical reaction of ground-state reactants $\text{Li}(^2S) + \text{NaLi}(X^1\Sigma^+) \rightarrow \text{Li}_2(X^1\Sigma_g^+) + \text{Na}(^2S)$.³⁹

We assume that both $\text{NaLi}(a^3\Sigma^+)$ molecules and Li atoms are prepared in their fully polarized electron spin states prior to the reaction, which is readily achievable experimentally.^{4,8,47} Thereby, the reaction complex is initialized in a state with the total electron spin projection $M_S = \pm \frac{3}{2}$, which corresponds to $S = \frac{3}{2}$. Following previous theoretical work,^{49,53,54} we assume the validity of the Wigner spin rule,^{7,43,55–57} which states that S , the total electron spin of the reaction complex, is conserved. This allows us to restrict attention to the quantum dynamics on a single adiabatic $1^4A'$ PES and neglect the intersystem crossing transitions to the low-spin $1^2A'$ and $2^2A'$ PESs, which exhibit a CI.³⁹ The CI could, in principle, affect the dynamics via intersystem crossing transitions mediated by weak S -nonconserving couplings between the $1^4A'$ PESs and the low-lying PESs due to, e.g., the intramolecular spin–spin interaction in NaLi .^{7,58} Model calculations show that such S -nonconserving pathways are typically suppressed by a factor of >10 compared to their S -conserving counterparts in chemical reactions of light atoms and molecules,^{7,36} although infrequent exceptions can occur at certain collision energies and magnetic fields. To rigorously quantify the effect of the doublet PESs and their CI, it is necessary to carry out quantum reactive scattering calculations, which explicitly account for the interactions between the high- and low-spin PESs ($1^4A'$, $1^2A'$, and $2^2A'$). At present, this is computationally unfeasible, but progress toward such calculations is currently underway in our laboratories.

We have used the multi-reference configuration interaction (MRCI) method^{59,60} to calculate the $1^4A'$ PES of the NaLi_2 trimer based on reference wave functions for the two lowest spin-polarized states, $1^4A'$ and $2^4A'$. These reference functions have been obtained from state-averaged multi-reference self-consistent field (MCSCF) calculations.^{61,62} The three valence electrons that describe the NaLi_2 trimer are correlated using an active space composed of 12 orbitals, where nine and three are of A' and A'' symmetry, respectively. The basis sets and

effective core and polarization potentials used for Na and Li atoms are described in detail in our recent work,³⁹ which was focused on the energetically lowest spin doublet states $1^2A'$ and $2^2A'$. We performed the electronic structure calculations using the MOLPRO package,⁶³ with further details given in the Supporting Information.⁶⁴ The PES for the $1^4A'$ electronic state of the Li_2Na trimer used in our reactive scattering calculations has the form

$$V_{1^4A'}(r_a, r_b, \alpha) = V_{1^4A'}^{\text{pairwise}}(r_a, r_b, \alpha) + \lambda V_{1^4A'}^{\text{3-body}}(r_a, r_b, \alpha) \quad (1)$$

where r_a and r_b denote the two NaLi bond lengths, α is the $\text{Li}(a)-\text{Na}-\text{Li}(b)$ bond angle, $V_{1^4A'}^{\text{pairwise}}(r_a, r_b, \alpha)$ is the three-atom pairwise (two-body) potential obtained by adding the spectroscopically accurate $\text{NaLi}(a^3\Sigma^+)$ and $\text{Li}_2(a^3\Sigma_u^+)$ dimer potentials from refs 7 and 65, and $V_{1^4A'}^{\text{3-body}}(r_a, r_b, \alpha)$ is the non-additive three-body contribution.⁶⁴ Scaling parameter λ is used below to explore the sensitivity of our results to small variations in the non-additive three-body part of the PES. Unless stated otherwise, we assume $\lambda = 1$.

Figure 1b shows contour plots of our $ab\ initio$ Li_2Na PES as a function of the Jacobi coordinates (R, r_{NaLi}) for several values of the Jacobi angle in the $\text{Li}-\text{NaLi}$ arrangement. The PES is barrierless, and the global minimum occurs at a θ of 105° in the $\text{Li} + \text{NaLi}$ arrangement ($R = 5.75 a_0$, and $r = 6.85 a_0$) as shown in the middle panel of Figure 1b. The PES depth counted from the minimum of the $\text{Li}_2(a^3\Sigma_u^+)$ product's potential energy curve is 3012 K. The exothermicity of the reaction $\text{Li} + \text{NaLi}(a^3\Sigma^+, v = 0, j = 0) \rightarrow \text{Li}_2(a^3\Sigma_u^+, v' = 0, j' = 0) + \text{Na}$ is ~ 94.9 K (~ 112.0 K), including (excluding) the zero-point energies of the reactants and products. This makes it possible for the reaction to occur at ultralow collision energies. Figure 1c shows the internal rovibrational energy levels of the reactants and products calculated from the accurate $ab\ initio$ potential energy curves of $\text{NaLi}(a^3\Sigma^+)$ and $\text{Li}_2(a^3\Sigma_u^+)$.^{7,65} In calculating the energy levels, we neglected the small splittings due to the fine and hyperfine structure of the reactants and products, as done in prior theoretical work on nonpolar alkali dimers.^{49,53,54} This is expected to be a

reasonable approximation for fully spin-polarized reactants.⁵⁴ In the limit of zero collision energy, a total of 18 rovibrational states of Li_2 are energetically accessible, including 15 states in the $v' = 0$ manifold ($j' = 0-14$) and three states in the $v' = 1$ manifold ($j' = 0-2$).

To study the quantum dynamics of the ultracold $\text{Li} + \text{NaLi} \rightarrow \text{Li}_2 + \text{Na}$ reaction, we use a rigorous quantum dynamics approach based on the adiabatically adjusting principal-axis frame hyperspherical (APH) coordinates as described in the Supporting Information.⁶⁴ Figure 2d shows the adiabatic eigenvalues $e_n^{lpq}(\rho_\xi)$ of the Li_2Na reaction complex calculated using the accurate *ab initio* PES (see the Supporting Information⁶⁴ for technical details). The corresponding fixed- ρ contour plots of the $1^4A'$ PES as a function of the polar and azimuthal hyperangles are displayed in panels a–c. The entire configuration space can be divided into three distinct regions. In the short-range region ($\rho = 8-15 a_0$), a strongly bound NaLi_2 reaction complex forms, and the different reaction arrangements are strongly coupled. The adiabatic energies range from -3000 K (near the PES minimum) to the three-body breakup threshold and above.

In the intermediate region ($\rho = 15-40 a_0$), the reactant and product arrangements, while still strongly coupled, begin to separate from one another. As shown in Figure 2c, at $\rho = 20 a_0$ there still exists a large region of configurational space between the reactant and product reaction arrangements (colored light blue) where the PES is large and negative. Thus, the reactive scattering wave function at $\rho = 20 a_0$ is still substantially delocalized between the reactant and product arrangements. This is true because the reactants and products of the $\text{Li} + \text{NaLi}(a^3\Sigma^+) \rightarrow \text{Li}_2(a^3\Sigma_u^+) + \text{Na}$ chemical reaction are weakly bound [van der Waals (vdW)] molecules held together by long-range dispersion forces, with binding energies not exceeding 300 K.^{66,67} This makes the vdW chemical reaction studied here significantly different from those of covalently bound molecules such as $\text{Li} + \text{NaLi}(X^1\Sigma^+) \rightarrow \text{Li}_2(X^1\Sigma_g^+) + \text{Na}$,^{39,40} where the separation of the reactant and product arrangements is essentially complete at much smaller ρ values of $\approx 10-15 a_0$. This persistence of reactive (interarrangement) couplings up to a large ρ is due to the proximity to the three-body breakup threshold and may be considered as a distinctive feature of quantum dynamics of vdW chemical reactions. We note that in three-body recombination reactions, which start above the three-body threshold, such interarrangement couplings occur even asymptotically at large ρ values.⁶⁸ Ultracold vdW reactions thus occupy an intermediate position between conventional chemical reactions, which take place at very close range ($\rho \leq 15 a_0$), and three-body recombination transitions (or chemical reactions of Feshbach molecules), which occur at very long range ($\rho \geq 100 a_0$).

The value of $\rho = 40 a_0$ marks the beginning of the long-range region, where the entrance and exit reaction arrangements are completely separated on the surface of a hypersphere by a barrier with a height of >200 K (note that this barrier does not correspond to an actual barrier in the reaction path). In the limit $\rho \rightarrow \infty$, different reaction arrangements become localized at specific hyperangles θ_ω which correspond to the minima of the diatomic molecule's potentials in each arrangement. The adiabatic curves computed without the three-body terms ($\lambda = 0$) are nearly identical to their three-body counterparts already at $\rho \geq 14 a_0$ as shown in the inset of Figure 2d. The three-body terms dominate at short range due to a conical

intersection between the ground and first excited quartet PESs.^{54,64,69}

Figure 3a shows the total rate of the $\text{Li} + \text{NaLi}(a^3\Sigma^+)$ chemical reaction, $K_{\text{tot}} = \sigma_r v$, where σ_r is the total reaction cross

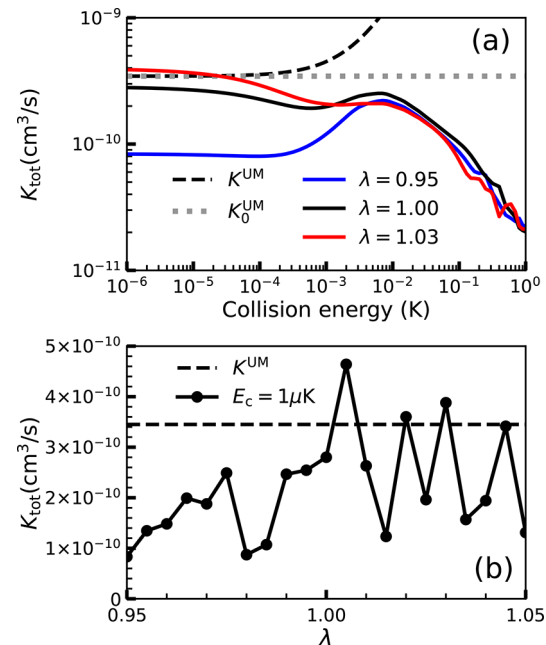


Figure 3. (a) Total rate coefficients for the $\text{Li} + \text{NaLi}(a^3\Sigma^+, v = 0, j = 0) \rightarrow \text{Li}_2(a^3\Sigma_u^+) + \text{Na}$ chemical reaction plotted as a function of collision energy for different values of PES scaling parameter λ . The universal rate K^{UM} (long dashed line) and its s-wave component K_0^{UM} (short dashed line) are shown. (b) Same as panel a at $E = 1 \mu\text{K}$ plotted as a function of λ .

section and $v = \hbar k/\mu$ is the collision velocity, calculated for several values of scaling parameter λ . The rate approaches a constant value in the s-wave limit of zero collision energy in keeping with the Wigner threshold law ($K_{\text{tot}} \simeq k^2$). Also plotted in Figure 3a is the total universal reaction rate calculated as $K^{\text{UM}} = K_0^{\text{UM}} + K_1^{\text{UM}}(E)$, where K_0^{UM} and $K_1^{\text{UM}}(E)$ are the s-wave and p-wave universal rates calculated as described in refs 35 and 41. These are evaluated under the assumption that all of the incoming flux is fully absorbed at short range (loss parameter $y = 1$), which leads to the same universal rate expression, parametrized by the long-range dispersion coefficient C_6 and the reduced mass for the collision, regardless of the details of short-range interactions^{35,41} (see the Supporting Information⁶⁴ for more details).

To obtain the universal rates, we calculated a C_6 value of 2891 au for the $\text{Li}-\text{NaLi}(a^3\Sigma^+)$ trimer using a high-level spin-restricted coupled-cluster method with single, double, and perturbative triple excitations RCCSD(T) and an aug-cc-pwCVQZ basis set with a bond length of NaLi at $9.0906 a_0$ corresponding to the average internuclear distance of $\text{NaLi}(a^3\Sigma^+, v = 0, j = 0)$.⁶⁴

A striking feature observed in Figure 3a is that the total reaction rate calculated using our exact quantum approach for $\lambda = 0.95$ ($K_{\text{tot}} = 8.33 \times 10^{-11} \text{ cm}^3/\text{s}$) is 4.1 times smaller than the universal rate (K_0^{UM}) of $3.45 \times 10^{-10} \text{ cm}^3/\text{s}$ in the s-wave regime. The reaction rate calculated with $\lambda = 1.03$ is 4.7 times larger than that calculated with $\lambda = 0.95$. This indicates that non-universal effects due to short-range reflection of the incident scattering flux^{7,8,35} (which appear because not all

short-range collisions result in irreversible loss due to, e.g., long-lived complex formation) can play a crucial role in the ultracold chemical reaction $\text{Li} + \text{NaLi}(a^3\Sigma^+) \rightarrow \text{Li}_2(a^3\Sigma_u^+) + \text{Na}$ despite the presence of a deep potential well. This stands in contrast to the behavior observed thus far in quantum scattering calculations on other ultracold atom–molecule insertion reactions.^{29,37,39,40,54} In particular, the chemical reactions of ground-state reactants such as $\text{K} + \text{KRb}(X^1\Sigma^+) \rightarrow \text{K}_2(X^1\Sigma_g^+) + \text{Rb}$,²⁹ $\text{Li} + \text{LiYb}(X^2\Sigma^+) \rightarrow \text{Li}_2(X^1\Sigma_g^+) + \text{Yb}(^1\text{S})$,³⁷ and $\text{Li} + \text{NaLi}(X^1\Sigma^+) \rightarrow \text{Li}_2(X^1\Sigma_g^+) + \text{Na}$ ^{39,40} have deep potential wells and populate a large number of product states but occur at rates very close (within 30%) to the universal rates. Figure 3a shows that the λ dependence of the reaction rate becomes progressively weaker at higher collision energies ($E_c > 10^{-2}$ K) as quantum interference effects are washed out by multiple partial wave contributions.

As shown in Figure 3b, the chemical reaction $\text{Li} + \text{NaLi}(a^3\Sigma^+)$ can display both nearly universal and highly non-universal dynamics depending on the value of scaling parameter λ in eq (1). The uncertainties in our calculated three-body PES can be estimated at $\pm 5\text{--}10\%$. Thus, while non-universal behavior cannot, at present, be predicted to occur with 100% certainty, the results shown in Figure 3b suggest that its likelihood is much higher than for the previously studied ultracold chemical reactions, such as $\text{Li} + \text{NaLi}(X^1\Sigma^+)$,³⁹ which did not show any significant deviations from universal behavior as a function of λ . Significantly, note that the numerical agreement of the reaction rate with the universal rate does not necessarily mean that the dynamics is described well by the UMs.

To further explore the variation of the rates with the short-range potential, we plot in Figure 4 the loss rate at the low

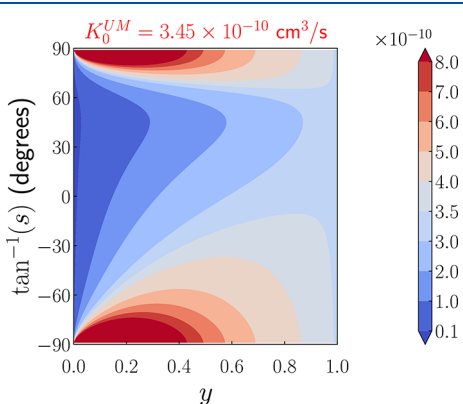


Figure 4. Contour plot of the s-wave loss rate (cubic centimeters per second) calculated using the UM³⁵ as a function of short-range loss parameter y ($0 \leq y \leq 1$) and the reduced scattering length $s = a/\bar{a}$. In the limit $y \rightarrow 1$, the rate become equal to the universal rate ($K_0^{\text{UM}} = 3.45 \times 10^{-10} \text{ cm}^3/\text{s}$) regardless of the value of s . The loss rate approaches zero as $y \rightarrow 0$.

energy limit using the UM of ref 35 as a function of short-range loss parameter y and the reduced scattering length $s = a/\bar{a}$, where \bar{a} is the mean scattering length given by the equation⁷⁰ $\bar{a} = [2\pi/\Gamma(1/4)^2](2\mu C_6/\hbar^2)^{1/4}$. We observe that for a large loss ($y > 0.8$) we are more likely to observe rates slightly above or below the universal value, as done in this work. In this regime, the small amount of incident flux reflected from the short range without reaction tends to interfere mostly destructively with the incoming flux. The underlying physics

is contained in the pole structure of the complex scattering length (see eq 11 of ref 35). On the contrary, when $y < 0.5$, observing the rates above the universal value becomes more and more likely, especially in the case of a large $|a|$ (i.e., near a scattering resonance). This is because the amount of reflected flux increases with a decrease in y , allowing for a more pronounced quantum interference between the incident and reflected fluxes. As mentioned by Idziaszek and Julienne,³⁵ the quantum interference effects in the UM are counterintuitive and will be the subject of further study.

To explain the strong variation of the ultracold $\text{Li} + \text{NaLi}(a^3\Sigma^+)$ reaction rate with λ shown in Figure 3, we recall (see above) that the reactants and products of this chemical reaction are weakly bound vdW molecules, whose binding energies do not exceed 300 K.⁶⁷ By contrast, the ultracold chemical reactions between alkali metal and alkaline earth atoms and molecules studied thus far occur between covalently bound molecules, with binding energies above 1000 K. As a result, the number of open reaction channels populated in these latter reactions [126 for $\text{Li} + \text{NaLi}(^1\text{X})$, 143 for $\text{K} + \text{KRb}$, and 1279 for $\text{Li} + \text{LiYb}$]^{29,38,39} is large compared to the 18 open channels in the $\text{Li} + \text{NaLi}(a^3\Sigma^+)$ chemical reaction studied here.

The total reaction rate is a sum of the individual state-to-state reaction rates, which fluctuate strongly as a function of λ . These state-to-state fluctuations average out in the total reaction rate, and the degree of averaging depends on the number of contributing state-to-state rates, which is equal to the number of open reaction channels. Because the number of open channels is much smaller for the ultracold $\text{Li} + \text{NaLi}(a^3\Sigma^+)$ vdW reaction, the averaging is not complete, and the total rate fluctuates strongly as a function of λ (see Figures S3 and S4 for the details of state-to-state rates). In contrast, the reactions of deeply bound reactants typically populate hundreds of final channels, ensuring nearly complete averaging of the individual state-to-state contributions to the total reaction rate, which then fluctuates only weakly with λ (see, e.g., Figure 12 of ref 39).

This suggests that experimental measurements of state-to-state reaction rates could be used to obtain insight into three-body interactions in triatomic reaction complexes such as NaLi_2 . In particular, if a sufficiently large set of experimental state-to-state rates becomes available, it may be possible to constrain the form of the three-body interaction (the value of λ) uniquely. Such state-to-state measurements have recently been carried out for the ultracold $\text{KRb} + \text{KRb} \rightarrow \text{K}_2 + \text{Rb}_2$ chemical reaction.¹⁸

The near-threshold density of states of the $\text{Li}-\text{NaLi}(a^3\Sigma^+)$ trimer can be approximated as $\rho \propto D_e^{3/2}/\sqrt{k_r k_R}$, where D_e is the dissociation energy measured from the minimum of the trimer PES and k_r and k_R are the harmonic force constants for the NaLi vibrational mode and for the motion along atom–molecule coordinate R , respectively.⁷¹ For the $\text{Li}+\text{NaLi}(^4\text{A}')$ reaction complex, we estimate the density of states as $\rho = 3.53 \text{ K}^{-1}$, which is 16.7 times lower than that of the ${}^{40}\text{K} + {}^{40}\text{K} {}^{87}\text{Rb}$ trimer ($\rho = 56.6 \text{ K}^{-1}$)⁷¹ (this calculation neglects the hyperfine structure of the reactants).

This is consistent with our calculations (see Figure 3b and Figure S.3a), which show that state-to-state reaction rates as a function of λ are strongly affected by resonance-like variations. This is because the 5–10% scaling of the three-body term leads to changes of a few hundreds of kelvin in the depth of the PES.

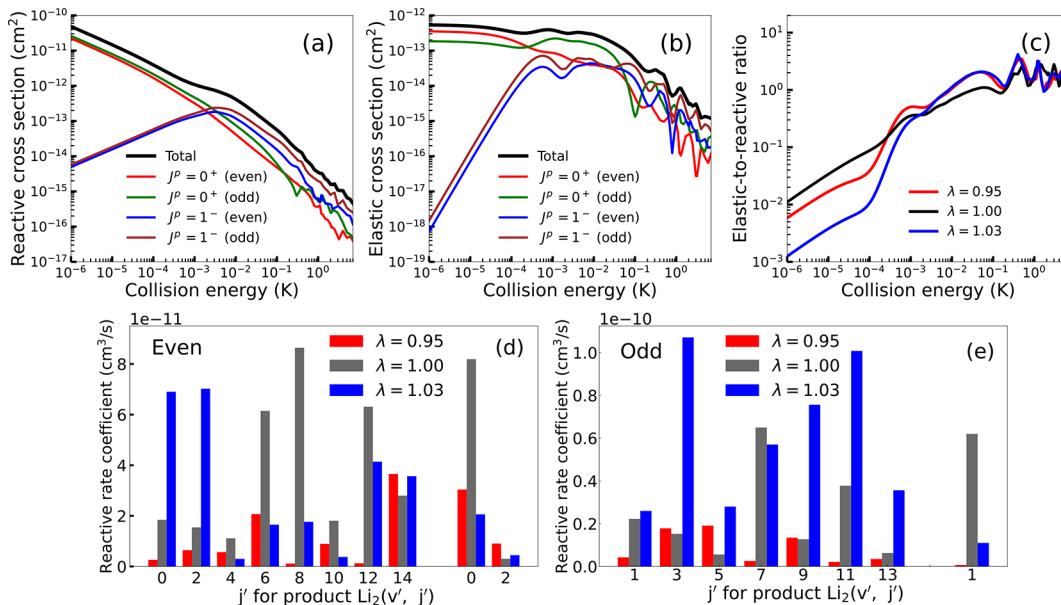


Figure 5. (a) Reactive and (b) elastic cross sections for the ultracold chemical reaction $\text{Li} + \text{NaLi}(v = 0, j = 0) \rightarrow \text{Li}_2 + \text{Na}$ plotted as a function of collision energy for different values of J , parity p , and exchange symmetry for $\lambda = 1$. The total integral cross sections (solid black lines) are obtained by summing the cross sections for even and odd ${}^6\text{Li}$ exchange symmetries multiplied by the statistical factors $1/3$ and $2/3$. These factors are the opposite of those used in previous calculations on the ground-state PESs^{37,39,40} because the $X^1\Sigma_g^+$ and $a^3\Sigma_u^+$ electronic states of ${}^6\text{Li}_2$ are even and odd with respect to the exchange of identical Li nuclei. (c) Ratio of elastic to reactive cross sections γ as a function of collision energy for different values of PES scaling parameter λ . Nascent product-state distributions of Li_2 over final rovibrational states (v', j') at $E = 1 \mu\text{K}$ for (d) even and (e) odd values of j' and three values of λ indicated in the legend. In panels d and e, the statistical factors for the exchange symmetries are not used.

It is likely that scattering resonances due to near-threshold bound states are responsible for the sensitivity, in which case spectroscopic experiments should provide important information about the true value of the three-body interaction. Because the total reaction rate is the sum of 18 independent state-to-state contributions, we expect that it will show variations on λ scales much finer than those shown in Figure 3b. While the λ grid interval used in this work is not fine enough to resolve the individual state-to-state oscillations, the potential role of near-threshold resonances in causing these oscillations is an important question to address in future work. In addition, it will be important to explore the sensitivity of state-to-state reaction rates to the anisotropy of the three-body interaction. Finally, the background values of reaction rates could be estimated by averaging the calculated λ -dependent rates over λ .⁷²

In Figure 5a, we plot the total integral cross section for the $\text{Li} + \text{NaLi}(a^3\Sigma^+, v = 0, j = 0)$ reaction (σ_r) as a function of collision energy for several lowest values of J , inversion parity ($p = \pm 1$), and identical Li nuclei exchange symmetry (even and odd). Both even and odd exchange symmetries are seen to contribute to the reactive cross section nearly equally in the s-wave regime ($l = 0$), and the p-wave contributions ($l = 1$) become important at $E > 3 \text{ mK}$. This behavior is consistent with the Wigner threshold scaling $\sigma_r \simeq E^{l-1/2}$, where l is the orbital angular momentum in the incident channel. The contribution of the even exchange symmetry to the elastic cross section shown in Figure 5b is significantly larger than that of the odd symmetry in the s-wave limit, indicating the importance of identical particle permutation symmetry in this reaction. Quantum interference between the Li exchange and non-exchange processes is likely responsible for this behavior as observed in the $\text{H} + \text{HD} \rightarrow \text{H} + \text{HD}$ ^{26,64,73} reaction (see also the Supporting Information⁶⁴). Above 3 mK, the p-wave

($l = 1$) elastic and reactive cross sections display several broad scattering resonances, whose contribution to the total reaction cross section is largely washed out, making it a smooth function of collision energy all the way up to 100 mK.

The ratio γ of the elastic to reactive cross sections displayed in Figure 5c decreases monotonically in the s-wave limit with a decrease in collision energy due to the different threshold scaling of the elastic and inelastic cross sections (see above) regardless of the value of λ . A large elastic-to-inelastic collision ratio ($\gamma \geq 10-100$) is an important prerequisite for sympathetic cooling, an experimental technique that relies on momentum-transfer (elastic) collisions of precooled molecules with ultracold atoms to further cool the molecules.⁷⁴⁻⁷⁷ Inelastic collisions and chemical reactions cause trap loss and heating, thereby limiting the efficiency of sympathetic cooling.⁷⁴⁻⁷⁷ The results shown in Figure 5c thus suggest that the chemical reaction $\text{Li} + \text{NaLi}(v = 0, j = 0) \rightarrow \text{Li}_2 + \text{Na}$ will prevent efficient sympathetic cooling of NaLi molecules via elastic collisions with spin-polarized Li atoms. It is worth noting that the efficient sympathetic cooling observed by Son et al.⁴⁸ in a trapped mixture of NaLi molecules with Na atoms would not be adversely affected by the chemical reaction $\text{Na} + \text{NaLi}(a^3\Sigma^+, v = 0, j = 0) \rightarrow \text{Na}_2(a^3\Sigma_u^+) + \text{Li}$ because it is endothermic and hence cannot occur at ultralow temperatures.⁷ Our results thus suggest that, to achieve efficient sympathetic cooling, the spin-conserving chemical reactions allowed by the Wigner spin rule should be made endothermic via, e.g., a proper choice of atomic collision partners.

Panels d and e of Figure 5 show nascent Li_2 product-state distributions over the final rovibrational states (v', j') at $E = 1 \mu\text{K}$ for even and odd exchange symmetries. The distributions are highly non-uniform for all λ values and exchange symmetries. The state-to-state reaction rates are highly sensitive to λ due to quantum interference and resonance

effects, which, however, are partially averaged out in the total reaction rate (see above).

In summary, motivated by recent experimental advances in measuring collisional properties of ultracold NaLi($a^3\Sigma^+$) molecules with alkali metal atoms,^{8,48} we have performed accurate *ab initio* and quantum scattering calculations on the prototypical vdW chemical reaction $\text{NaLi}(a^3\Sigma^+) + \text{Li} \rightarrow \text{Li}_2(a^3\Sigma_u^+) + \text{Na}$, which is energetically allowed at ultralow temperatures. We found that the calculated total reaction rate is highly sensitive to tiny changes in the interaction PES (by a factor of ≈ 4), which suggests marked deviations from universal behavior.

These results are unprecedented for an ultracold chemical reaction involving a polar molecule. Indeed, all quantum scattering calculations performed thus far^{29,31,38,39} showed that such reactions do not deviate by $>30\%$ from the universal behavior (see, e.g., Figure 4 of ref 38 and Figure 7 of ref 39). Therefore, the chemical reaction $\text{Li} + \text{NaLi}(a^3\Sigma^+) \rightarrow \text{Li}_2 + \text{Na}$ could be a good candidate for the experimental study of non-universal chemistry in an optically trapped mixture of NaLi($a^3\Sigma^+$) molecules and Li atoms.

A key result of this work is the first observation of strongly non-universal dynamics in an ultracold barrierless insertion reaction involving a polar molecule. The breakdown of universality is remarkable for several reasons. First, it gives us a rare glimpse into a new regime of ultracold chemical dynamics, which cannot be described by simple universal models even at a qualitative level. Second, non-universal dynamics are sensitive to fine details of the underlying PES of the reaction complex. As such, measuring state-resolved reaction rates beyond the universal limit, as done in recent pioneering experiments,^{8,46} will enable high-precision characterization of intermolecular interactions within metastable reaction complexes, a much sought-after goal of ultracold chemistry.^{3,4,43}

Our results also have significant implications for molecular sympathetic cooling of alkali dimer molecules by collisions with ultracold atoms in a magnetic trap. The large reaction rates of spin-polarized reactants observed here (see Figure 5c) imply that preparing the reactants in their fully spin-polarized initial states will not prevent rapid collisional losses if spin-conserving atom–molecule chemical reactions [such as the $\text{Li} + \text{NaLi}(a^3\Sigma^+)$ reaction explored here] are energetically allowed. This leads to a general design principle for choosing ultracold atom–molecule systems suitable for sympathetic cooling experiments: avoid spin-conserving chemical reactions by choosing the coolant atom in such a way as to make the reaction endothermic and, hence, energetically forbidden at ultralow temperatures.

■ ASSOCIATED CONTENT

Data Availability Statement

The data that support the findings of this study are available within the article and its [Supporting Information](#). Data are also available from the authors upon reasonable request.

SI Supporting Information

The Supporting Information is available free of charge at <https://pubs.acs.org/doi/10.1021/acs.jpcllett.3c00159>.

Details of *ab initio* calculations of the ${}^4\text{A}'$ PES of the Li_2Na trimer and technical details of quantum reactive scattering calculations ([PDF](#))

■ AUTHOR INFORMATION

Corresponding Authors

Paul Brumer – *Chemical Physics Theory Group, Department of Chemistry, and Center for Quantum Information and Quantum Control, University of Toronto, Toronto, Ontario M5S 3H6, Canada;* [ORCID iD](https://orcid.org/0000-0002-4763-2393); Email: paul.brumer@utoronto.ca

Timur V. Tscherbul – *Department of Physics, University of Nevada, Reno, Nevada 89557, United States;* [ORCID iD](https://orcid.org/0000-0001-5689-040X); Email: ttucherbul@unr.edu

Authors

Masato Morita – *Chemical Physics Theory Group, Department of Chemistry, and Center for Quantum Information and Quantum Control, University of Toronto, Toronto, Ontario M5S 3H6, Canada*

Brian K. Kendrick – *Theoretical Division (T-1, MS B221), Los Alamos National Laboratory, Los Alamos, New Mexico 87545, United States;* [ORCID iD](https://orcid.org/0000-0003-1806-9172)

Jacek Kłos – *Joint Quantum Institute, University of Maryland, College Park, Maryland 20742, United States; Department of Physics, Temple University, Philadelphia, Pennsylvania 19122, United States;* [ORCID iD](https://orcid.org/0000-0002-7407-303X)

Svetlana Kotchigova – *Department of Physics, Temple University, Philadelphia, Pennsylvania 19122, United States;* [ORCID iD](https://orcid.org/0000-0003-0580-3788)

Complete contact information is available at:
<https://pubs.acs.org/10.1021/acs.jpcllett.3c00159>

Notes

The authors declare no competing financial interest.

■ ACKNOWLEDGMENTS

M.M. thanks Dr. Pablo G. Jambrina for useful discussions. This work was supported by the National Science Foundation (NSF) through the CAREER program (PHY-2045681) and by the U.S. Air Force Office for Scientific Research (AFOSR) under Contracts FA9550-19-1-0312 and FA9550-22-1-0361 to P.B. and T.V.T. J.K. and S.K. acknowledge support from the U.S. AFOSR under Grant FA9550-21-1-0153 and the NSF under Grant PHY-1908634. B.K.K. acknowledges that part of this work was done under the auspices of the U.S. Department of Energy under Project 20170221ER of the Laboratory Directed Research and Development Program at Los Alamos National Laboratory. This work used resources provided by the Los Alamos National Laboratory Institutional Computing Program. Los Alamos National Laboratory is operated by Triad National Security, LLC, for the National Nuclear Security Administration of the U.S. Department of Energy (Contract 89233218CNA000001).

■ REFERENCES

- (1) Carr, L. D.; DeMille, D.; Krems, R. V.; Ye, J. Cold and ultracold molecules: Science, technology and applications. *New J. Phys.* **2009**, *11*, 055049.
- (2) Herschbach, D. Molecular collisions, from warm to ultracold. *Faraday Discuss.* **2009**, *142*, 9–23.
- (3) Balakrishnan, N. Perspective: Ultracold molecules and the dawn of cold controlled chemistry. *J. Chem. Phys.* **2016**, *145*, 150901.
- (4) Bohn, J. L.; Rey, A. M.; Ye, J. Cold molecules: Progress in quantum engineering of chemistry and quantum matter. *Science* **2017**, *357*, 1002–1010.

- (5) Liu, Y.; Ni, K.-K. Bimolecular chemistry in the ultracold regime. *Annu. Rev. Phys. Chem.* **2022**, *73*, 73–96.
- (6) Tscherbul, T. V.; Krems, R. V. Tuning bimolecular chemical reactions by electric fields. *Phys. Rev. Lett.* **2015**, *115*, 023201.
- (7) Hermsmeier, R.; Klos, J.; Kotochigova, S.; Tscherbul, T. V. Quantum spin state selectivity and magnetic tuning of ultracold chemical reactions of triplet alkali-metal dimers with alkali-metal atoms. *Phys. Rev. Lett.* **2021**, *127*, 103402.
- (8) Son, H.; Park, J. J.; Lu, Y.-K.; Jamison, A. O.; Karman, T.; Ketterle, W. Control of reactive collisions by quantum interference. *Science* **2022**, *375*, 1006–1010.
- (9) Orzel, C.; Walhout, M.; Sterr, U.; Julienne, P. S.; Rolston, S. L. Spin polarization and quantum-statistical effects in ultracold ionizing collisions. *Phys. Rev. A* **1999**, *59*, 1926–1935.
- (10) Mody, A.; Haggerty, M.; Doyle, J. M.; Heller, E. J. No-sticking effect and quantum reflection in ultracold collisions. *Phys. Rev. B* **2001**, *64*, 085418.
- (11) Bai, Y.-P.; Li, J.-L.; Wang, G.-R.; Cong, S.-L. Model for investigating quantum reflection and quantum coherence in ultracold molecular collisions. *Phys. Rev. A* **2019**, *100*, 012705.
- (12) Ni, K.-K.; Ospelkaus, S.; Wang, D.; Quéméner, G.; Neyenhuis, B.; de Miranda, M. H. G.; Bohn, J. L.; Ye, J.; Jin, D. S. Dipolar collisions of polar molecules in the quantum regime. *Nature (London)* **2010**, *464*, 1324–1328.
- (13) Quéméner, G.; Julienne, P. S. Ultracold molecules under control! *Chem. Rev.* **2012**, *112*, 4949–5011.
- (14) Devolder, A.; Tscherbul, T. V.; Brumer, P. Coherent control of reactive scattering at low temperatures: Signatures of quantum interference in the differential cross sections for F+H₂ and F+HD. *Phys. Rev. A* **2020**, *102*, 031303.
- (15) Devolder, A.; Brumer, P.; Tscherbul, T. V. Complete quantum coherent control of ultracold molecular collisions. *Phys. Rev. Lett.* **2021**, *126*, 153403.
- (16) Hu, M.-G.; Liu, Y.; Grimes, D. D.; Lin, Y.-W.; Gheorghe, A. H.; Vexiau, R.; Boulofa-Maafa, N.; Dulieu, O.; Rosenband, T.; Ni, K.-K. Direct observation of bimolecular reactions of ultracold KRb molecules. *Science* **2019**, *366*, 1111–1115.
- (17) Liu, Y.; Hu, M.-G.; Nichols, M. A.; Grimes, D. D.; Karman, T.; Guo, H.; Ni, K.-K. Photo-excitation of long-lived transient intermediates in ultracold reactions. *Nat. Phys.* **2020**, *16*, 1132–1136.
- (18) Liu, Y.; Hu, M.-G.; Nichols, M. A.; Yang, D.; Xie, D.; Guo, H.; Ni, K.-K. Precision test of statistical dynamics with state-to-state ultracold chemistry. *Nature* **2021**, *593*, 379–384.
- (19) Weck, P. F.; Balakrishnan, N. Importance of long-range interactions in chemical reactions at cold and ultracold temperatures. *Int. Rev. Phys. Chem.* **2006**, *25*, 283–311.
- (20) Krems, R. V. *Molecules in electromagnetic fields: from ultracold physics to controlled chemistry*; John Wiley & Sons, Ltd.: Hoboken, NJ, 2018.
- (21) Balakrishnan, N.; Dalgarno, A. Chemistry at ultracold temperatures. *Chem. Phys. Lett.* **2001**, *341*, 652–656.
- (22) Tizniti, M.; Le Picard, S. D.; Lique, F.; Berteloite, C.; Canosa, A.; Alexander, M. H.; Sims, I. R. The rate of the F + H₂ reaction at very low temperatures. *Nat. Chem.* **2014**, *6*, 141–145.
- (23) De Fazio, D.; Aquilanti, V.; Cavalli, S. Quantum dynamics and kinetics of the F + H₂ and F + D₂ reactions at low and ultra-low temperatures. *Front. Chem.* **2019**, *7*, 328–328.
- (24) Simbotin, I.; Ghosal, S.; Côté, R. A case study in ultracold reactive scattering: D + H₂. *Phys. Chem. Chem. Phys.* **2011**, *13*, 19148–19155.
- (25) Simbotin, I.; Côté, R. Effect of nuclear spin symmetry in cold and ultracold reactions: D + para/ortho-H₂. *New J. Phys.* **2015**, *17*, 065003.
- (26) Kendrick, B. K.; Hazra, J.; Balakrishnan, N. Geometric phase appears in the ultracold hydrogen exchange reaction. *Phys. Rev. Lett.* **2015**, *115*, 153201.
- (27) Kendrick, B. K. Non-adiabatic quantum reactive scattering calculations for the ultracold hydrogen exchange reaction: H + H₂(v = 4–8, j = 0) → H + H₂(v',j'). *Chem. Phys.* **2018**, *515*, 387–399.
- (28) Kendrick, B. K. Nonadiabatic ultracold quantum reactive scattering of hydrogen with vibrationally excited HD(v = 5–9). *J. Phys. Chem. A* **2019**, *123*, 9919–9933.
- (29) Croft, J. F. E.; Makrides, C.; Li, M.; Petrov, A.; Kendrick, B. K.; Balakrishnan, N.; Kotochigova, S. Universality and chaoticity in ultracold K + KRb chemical reactions. *Nat. Commun.* **2017**, *8*, 15897.
- (30) Croft, J. F. E.; Balakrishnan, N.; Kendrick, B. K. Long-lived complexes and signatures of chaos in ultracold K₂+Rb collisions. *Phys. Rev. A* **2017**, *96*, 062707.
- (31) Ospelkaus, S.; Ni, K.-K.; Wang, D.; de Miranda, M. H. G.; Neyenhuis, B.; Quéméner, G.; Julienne, P. S.; Bohn, J. L.; Jin, D. S.; Ye, J. Quantum-state controlled chemical reactions of ultracold KRb molecules. *Science* **2010**, *327*, 853–857.
- (32) A notable exception is vibrational excitation of the reactant molecule, for which abstraction reactions can also become barrierless and exhibit a potential well [e.g., H(D) + H₂(v ≥ 5)] (see refs 25, 27, and 28).
- (33) Quéméner, G.; Bohn, J. L. Strong dependence of ultracold chemical rates on electric dipole moments. *Phys. Rev. A* **2010**, *81*, 022702.
- (34) Kotochigova, S. Dispersion interactions and reactive collisions of ultracold polar molecules. *New J. Phys.* **2010**, *12*, 073041.
- (35) Idziaszek, Z.; Julienne, P. S. Universal rate constants for reactive collisions of ultracold molecules. *Phys. Rev. Lett.* **2010**, *104*, 113202.
- (36) Tscherbul, T. V.; Klos, J. Magnetic tuning of ultracold barrierless chemical reactions. *Phys. Rev. Research* **2020**, *2*, 013117.
- (37) Makrides, C.; Hazra, J.; Pradhan, G. B.; Petrov, A.; Kendrick, B. K.; González-Lezana, T.; Balakrishnan, N.; Kotochigova, S. Ultracold chemistry with alkali-metal–rare-earth molecules. *Phys. Rev. A* **2015**, *91*, 012708.
- (38) Li, H.; Li, M.; Makrides, C.; Petrov, A.; Kotochigova, S. Universal scattering of ultracold atoms and molecules in optical potentials. *Atoms* **2019**, *7*, 36.
- (39) Kendrick, B. K.; Li, H.; Li, M.; Kotochigova, S.; Croft, J. F. E.; Balakrishnan, N. Non-adiabatic quantum interference in the ultracold Li + LiNa → Li₂ + Na reaction. *Phys. Chem. Chem. Phys.* **2021**, *23*, 5096–5112.
- (40) Kendrick, B. K. Quantum reactive scattering calculations for the cold and ultracold Li+LiNa → Li₂+Na reaction. *J. Chem. Phys.* **2021**, *154*, 124303.
- (41) Julienne, P. S.; Hanna, T. M.; Idziaszek, Z. Universal ultracold collision rates for polar molecules of two alkali-metal atoms. *Phys. Chem. Chem. Phys.* **2011**, *13*, 19114–19124.
- (42) Frye, M. D.; Julienne, P. S.; Hutson, J. M. Cold atomic and molecular collisions: Approaching the universal loss regime. *New J. Phys.* **2015**, *17*, 045019.
- (43) Krems, R. V. Cold Controlled Chemistry. *Phys. Chem. Chem. Phys.* **2008**, *10*, 4079–4092.
- (44) Wang, T. T.; Heo, M.-S.; Rvachov, T. M.; Cotta, D. A.; Ketterle, W. Deviation from universality in collisions of ultracold ⁶Li₂ molecules. *Phys. Rev. Lett.* **2013**, *110*, 173203.
- (45) Yang, H.; Zhang, D.-C.; Liu, L.; Liu, Y.-X.; Nan, J.; Zhao, B.; Pan, J.-W. Observation of magnetically tunable Feshbach resonances in ultracold ²³Na⁴⁰K + ⁴⁰K collisions. *Science* **2019**, *363*, 261.
- (46) Park, J. J.; Lu, Y.-K.; Jamison, A. O.; Tscherbul, T. V.; Ketterle, W. A Feshbach resonance in collisions between triplet ground-state molecules. *Nature* **2023**, *614*, 54–58.
- (47) Rvachov, T. M.; Son, H.; Sommer, A. T.; Ebadi, S.; Park, J. J.; Zwierlein, M. W.; Ketterle, W.; Jamison, A. O. Long-lived ultracold molecules with electric and magnetic dipole moments. *Phys. Rev. Lett.* **2017**, *119*, 143001.
- (48) Son, H.; Park, J. J.; Ketterle, W.; Jamison, A. O. Collisional cooling of ultracold molecules. *Nature* **2020**, *580*, 197–200.
- (49) Cvitaš, M. T.; Soldán, P.; Hutson, J. M.; Honvárt, P.; Launay, J.-M. Ultracold Li + Li₂ collisions: Bosonic and fermionic cases. *Phys. Rev. Lett.* **2005**, *94*, 033201.
- (50) Cvitaš, M. T.; Soldán, P.; Hutson, J. M.; Honvárt, P.; Launay, J.-M. Interactions and dynamics in Li + Li₂ ultracold collisions. *J. Chem. Phys.* **2007**, *127*, 074302.

- (51) Soldán, P.; Cvitaš, M. T.; Hutson, J. M.; Honvau, P.; Launay, J.-M. Quantum dynamics of ultracold Na + Na₂ collisions. *Phys. Rev. Lett.* **2002**, *89*, 153201.
- (52) Quéméner, G.; Honvau, P.; Launay, J.-M.; Soldán, P.; Potter, D. E.; Hutson, J. M. Ultracold quantum dynamics: Spin-polarized K + K₂ collisions with three identical bosons or fermions. *Phys. Rev. A* **2005**, *71*, 032722.
- (53) Cvitaš, M. T.; Soldán, P.; Hutson, J. M.; Honvau, P.; Launay, J.-M. Ultracold collisions involving heteronuclear alkali metal dimers. *Phys. Rev. Lett.* **2005**, *94*, 200402.
- (54) Hutson, J. M.; Soldán, P. Molecular collisions in ultracold atomic gases. *Int. Rev. Phys. Chem.* **2007**, *26*, 1–28.
- (55) Moore, J. H. Investigation of the Wigner spin rule in collisions of N⁺ with He, Ne, Ar, N₂, and O₂. *Phys. Rev. A* **1973**, *8*, 2359–2362.
- (56) Tscherbul, T. V.; Krems, R. V. Controlling electronic spin relaxation of cold molecules with electric fields. *Phys. Rev. Lett.* **2006**, *97*, 083201.
- (57) Haze, S.; D'Incao, J. P.; Dorer, D.; Deiß, M.; Tiemann, E.; Julienne, P. S.; Denschlag, J. H. Spin-conservation propensity rule for three-body recombination of ultracold Rb atoms. *Phys. Rev. Lett.* **2022**, *128*, 133401.
- (58) Abrahamsson, E.; Tscherbul, T. V.; Krems, R. V. Inelastic collisions of cold polar molecules in nonparallel electric and magnetic fields. *J. Chem. Phys.* **2007**, *127*, 044302.
- (59) Knowles, P. J.; Werner, H.-J. An efficient method for the evaluation of coupling coefficients in configuration interaction calculations. *Chem. Phys. Lett.* **1988**, *145*, 514–522.
- (60) Werner, H.-J.; Knowles, P. J. An efficient internally contracted multiconfiguration–reference configuration interaction method. *J. Chem. Phys.* **1988**, *89*, 5803–5814.
- (61) Knowles, P. J.; Werner, H.-J. An efficient second-order MC SCF method for long configuration expansions. *Chem. Phys. Lett.* **1985**, *115*, 259–267.
- (62) Werner, H.-J.; Knowles, P. J. A second order multiconfiguration SCF procedure with optimum convergence. *J. Chem. Phys.* **1985**, *82*, 5053–5063.
- (63) Werner, H.-J.; et al. *MOLPRO, version 2015.1, a package of ab initio programs*; 2015.
- (64) See the [Supporting Information](#) for details of our *ab initio* and quantum reactive scattering calculations, including convergence tests, and for state-to-state reaction rates influenced by the potential scaling.
- (65) Lesiuk, M.; Musial, M.; Moszynski, R. Potential-energy curve for the a³Σ_u⁺ state of a lithium dimer with Slater-type orbitals. *Phys. Rev. A* **2020**, *102*, 062806.
- (66) Parker, G. A.; Walker, R. B.; Kendrick, B. K.; T Pack, R. Accurate quantum calculations on three-body collisions in recombination and collision-induced dissociation. I. Converged probabilities for the H+Ne₂ system. *J. Chem. Phys.* **2002**, *117*, 6083–6102.
- (67) Gronowski, M.; Koza, A. M.; Tomza, M. Ab initio properties of the NaLi molecule in the a³Σ⁺ electronic state. *Phys. Rev. A* **2020**, *102*, 020801.
- (68) D'Incao, J. P. Few-body physics in resonantly interacting ultracold quantum gases. *J. Phys. B* **2018**, *51*, 043001.
- (69) Colavecchia, F. D.; Burke, J. P.; Stevens, W. J.; Salazar, M. R.; Parker, G. A.; T Pack, R. The potential energy surface for spin-aligned Li₃ and the potential energy curve for spin-aligned Li₂. *J. Chem. Phys.* **2003**, *118*, 5484–5495.
- (70) Gribakin, G. F.; Flambaum, V. V. Calculation of the scattering length in atomic collisions using the semiclassical approximation. *Phys. Rev. A* **1993**, *48*, 546–553.
- (71) Frye, M. D.; Hutson, J. M. Complexes formed in collisions between ultracold alkali-metal diatomic molecules and atoms. *New J. Phys.* **2021**, *23*, 125008.
- (72) Morita, M.; Krems, R. V.; Tscherbul, T. V. Universal probability distributions of scattering observables in ultracold molecular collisions. *Phys. Rev. Lett.* **2019**, *123*, 013401.
- (73) Croft, J. F. E.; Hazra, J.; Balakrishnan, N.; Kendrick, B. K. Symmetry and the geometric phase in ultracold hydrogen-exchange reactions. *J. Chem. Phys.* **2017**, *147*, 074302.
- (74) Lara, M.; Bohn, J. L.; Potter, D.; Soldán, P.; Hutson, J. M. Ultracold Rb-OH collisions and prospects for sympathetic cooling. *Phys. Rev. Lett.* **2006**, *97*, 183201.
- (75) Tscherbul, T. V.; Klos, J.; Buchachenko, A. A. Ultracold spin-polarized mixtures of ²Σ molecules with S-state atoms: Collisional stability and implications for sympathetic cooling. *Phys. Rev. A* **2011**, *84*, 040701.
- (76) Morita, M.; Klos, J.; Buchachenko, A. A.; Tscherbul, T. V. Cold collisions of heavy ²Σ molecules with alkali-metal atoms in a magnetic field: Ab initio analysis and prospects for sympathetic cooling of SrOH(²Σ⁺) by Li(²S). *Phys. Rev. A* **2017**, *95*, 063421.
- (77) Morita, M.; Kosicki, M. B.; Żuchowski, P. S.; Tscherbul, T. V. Atom-molecule collisions, spin relaxation, and sympathetic cooling in an ultracold spin-polarized Rb(²S)–SrF(²Σ⁺) mixture. *Phys. Rev. A* **2018**, *98*, 042702.

□ Recommended by ACS

Recombination of N Atoms in a Manifold of Electronic States Simulated by Time-Reversed Nonadiabatic Photodissociation Dynamics of N₂

Natalia Gelfand, Raphael D. Levine, et al.

MAY 11, 2023

THE JOURNAL OF PHYSICAL CHEMISTRY LETTERS

READ ▶

Signatures of Reaction Mechanisms Encoded in the Vibrational Population Distribution of Small-Molecule Products: Photodissociation of Symmetric-Triazine Using...

Piyush Mishra, Robert W. Field, et al.

APRIL 11, 2023

THE JOURNAL OF PHYSICAL CHEMISTRY LETTERS

READ ▶

Dissociation Dynamics of Anionic Nitrogen Dioxide in the Low-Lying Resonant States

Jingchen Xie, Shan Xi Tian, et al.

JANUARY 12, 2023

THE JOURNAL OF PHYSICAL CHEMISTRY LETTERS

READ ▶

Infrared Spectroscopy of (Benzene-H₂S-X_n)⁺, X = H₂O (n = 1 and 2) and CH₃OH (n = 1), Radical Cation Clusters: Microsolvation Effects on the S-π Hemibond

Takeru Kato and Asuka Fujii

JANUARY 13, 2023

THE JOURNAL OF PHYSICAL CHEMISTRY A

READ ▶

Get More Suggestions >